2025 IMEKO TC26 International Conference on
Metrology for Archaeology and Cultural Heritage
Bergamo, Italy, October 15-17, 2025

Walls of the Castle of Alcácer do Sal – Contribution to the Study of Mortars in Military Architecture

M. Almeida[1], M. T. Pinheiro-Alves[2], P. Moita[3], C. Galacho[4]

[1] *University of Évora, Escola de Artes, Largo dos Colegiais 2, 7004-516, Évora, Portugal.* maria.almeida93@hotmail.com.
[2] *University of Évora, Escola de Artes, Largo dos Colegiais 2, 7004-516, Évora, Portugal.* tpa@uevora.pt.
[3]*Geoscience Department of School of Science and Technology, University of Évora, Rua Romão Ramalho 59, 7000-671 Évora, HERCULES Laboratory, IN2PAST Laboratory, Portugal.* pmoita@uevora.pt.
[4]*Chemistry and Biochemistry Department of School of Sciences and Technology, University of Évora, Rua Romão Ramalho 59, 7000-671 Évora, HERCULES Laboratory, IN2PAST Laboratory, Portugal.* pcg@uevora.pt.

Abstract – **The strategic location of Alcácer do Sal, on the banks of the Sado River and in a region rich in natural resources, explains the various occupations of this territory throughout history. However, it was the influence of the Muslim occupation (715–1217) that stood out the most, still visible today through archaeological remains, the town's name, and, in this case study, the castle walls (11th–12th centuries), which have undergone several interventions over time.**

A visual inspection of the walls was conducted to assess their current condition. This revealed that the main causes of deterioration are related to water infiltration due to insufficient maintenance, lack of proper drainage, and the absence of protective elements such as coping. These issues have led to the loss of render adhesion, biological colonization, and material disintegration in several areas.

The mortar samples were characterized using a multi-analytical approach, including Optical Microscopy (stereo zoom and petrographic microscope), X-ray Diffraction, Scanning Electron Microscopy with Energy Dispersive X-ray Spectroscopy, Thermogravimetric Analysis, acid attack, and granulometric analysis. The results indicate that the mortars have similar compositions in terms of raw materials and likely provenance. An intervention strategy was proposed to address the identified pathologies and support future conservation efforts.

Keywords: Alcácer do Sal, military architecture, conservation, mortars, materials characterization.

I. INTRODUCTION

The fortification walls of Alcácer do Sal are the result of multiple stages of improvement, reformulation, consolidation, and restoration, from the Middle Ages to the present day. Beginning with the construction of a fortified palace in the 9th century, they were later adapted to house the Palace of the Order of Santiago in the 13th century, followed by the construction of the Aracoeli Carmelite Convent in the 16th century, and finally converted into the current Pousada D. Afonso II, inaugurated in 1998. Based on the historical investigation of the site's military architecture and its heritage value, the present case study had as its main objectives the visual inspection of the site, the collection of samples from different sections of the walls—taking into account their state of conservation and the date of their last intervention—the laboratory analysis of the collected samples to identify and characterise the raw materials (the aggregate, binder, and additives) that were used for the production of the mortars, determine the provenance of the raw materials, and to study the technology employed for the production of the mortars, and finally, the proposal of strategies for their conservation.

The methodology involved defining the areas for analysis through an on-site visit carried out with the collaboration of heritage authorities, leading to the selection of five wall sectors, each with distinct characteristics and intervention histories. These zones,

dating from the 13th to the 20th century, presented varying states of conservation. A total of 18 samples of render mortars were collected across these five areas (Fig. 1). Visual inspection and anomaly mapping were conducted on-site, with photographic documentation, material observations, and structural measurements.

Fig. 1. Sample collection areas:

- *zone 1 (ALC 1A, ALC 1B)*
- *zone 2 (ALC2E, ALC2I, ALC3, ALC4E, ALC4I, ALC5)*
- *zone 3 (ALC6E, ALC6I, ALC7E, ALC7I)*
- *zone 4 (ALC8E)*
- *zone 5 ((ALC9E, ALC9I, ALC10R, ALC10T, ALC11EE, ALC11EI, ALC11I)*

The methodology used for the characterization of the mortars comprises a diverse set of analytical techniques that complement each other.

The results, combined with the observed pathologies, supported the proposal of a conservation intervention strategy adapted to the specific condition of each wall section.

II. CHARACTERIZATION OF MORTARS: A MULTIDISCIPLINARY METHODOLOGY

The characterization of mortars from Alcácer do Sal (tab.1) was conducted at the HERCULES Laboratory using a comprehensive and multidisciplinary methodology that integrated various analytical techniques to evaluate their textural, mineralogical, chemical, and microstructural properties. The primary objective was to determine the composition and state of preservation of the samples. The methodology began with a visual inspection of each sample to document color, aggregate distribution, and the presence of stratigraphy.

SAMPLE	PERIOD	LOCATION
ALC1A|B	séc. XI - XIII	zone 1
ALC2|3|4|5	1966	zone 2
ALC6|7	1985	Zone3
ALC8	1959	Zone4
ALC9|10|11	1972	Zone4

Tab. 1. Samples under study: period and location.

Approximately 10 g of each sample were processed in a planetary mill (500 rpm, 10 min) to obtain a global fraction (GF), which was essential for the mineralogical analyse. Samples were also observed under a stereomicroscope (Leica M205-C) and a polarized light microscope (Leica DM2500 P, under PPL and XPL) to identify morphology, aggregate types, and layer structure. Sample fragments were also embedded in epoxy resin, sectioned, and polished for microstructural analysis. The preparation of thin sections followed the Struers TS method, and their quality was confirmed under polarized light.

Powder X-Ray Diffraction (XRD) was used to identify the crystalline mineral phases. The analyses were performed on a Bruker AXS D8 Discover diffractometer with CuKα radiation (λ = 1.5406 Å), operating at 40 kV and 40 mA, with a scan from 3° to 75° 2θ. Thermogravimetric Analysis (TGA) was conducted on global sample fractions (approximately 25–30 mg) using a STA 449 F3 Jupiter (NETZSCH). The analysis was performed under a nitrogen atmosphere (70 mL/min), with heating from 40 to 1000°C at a rate of 10°C/min. This technique allowed for the quantification of carbonate content based on the weight loss observed between 600–900°C.

Scanning Electron Microscopy with Energy Dispersive X-ray Spectroscopy (SEM-EDS) was applied to polished cross-sections for microstructural and elemental characterization. The analyses were carried out on a HITACHI S-3700N with a Bruker XFlash 5010 (SDD), enabling high-magnification imaging (BSE mode), elemental analysis, and elemental mapping to characterize binder-aggregate relationships.

Granulometric analysis of the aggregates was performed following an acid attack with diluted HCl (1:3). Two 10 g portions of each sample were treated to separate the soluble and insoluble fractions. The insoluble residues were filtered, dried, weighed, and sieved (RETSCH, ASTM E11 sieves) to determine the size distribution of the aggregate particles.

III. RESULTS

Based on visual and stereo microscopy observations, the samples were grouped according to their binder color and aggregate characteristics. Most samples presented a homogeneous binder, ranging from light to dark brown (fig.2). Exceptions include samples ALC1A and ALC1B (Zone 1) with black-colored binders, ALC8E (Zone 4) with a whitish tone, and ALC10TR (Zone 5) with a greyish lower layer (fig.3). These chromatic differences may indicate construction in distinct chronological phases.

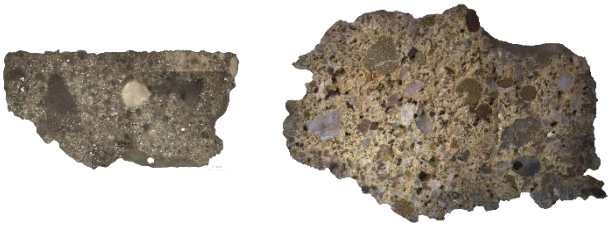

Fig. 2. Examples of samples (ALC3, ALC6) with brown homogeneous binder.

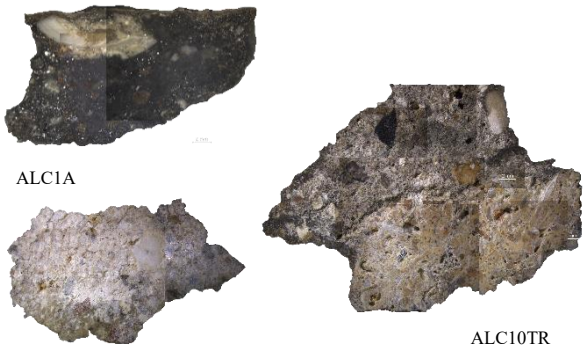

Fig. 3. Samples with different binder colors.

Regarding aggregate morphology and size, the samples can be broadly divided into two groups. Group 1 (Zones 1 and 2) shows porous textures with small, rounded aggregates, including shell fragments (ALC1A) and ceramic inclusions (ALC2E) (fig.4). Group 2 (Zones 3, 4, and 5) is more heterogeneous, with a variety of aggregate sizes and shapes, including angular and sub-angular grains.

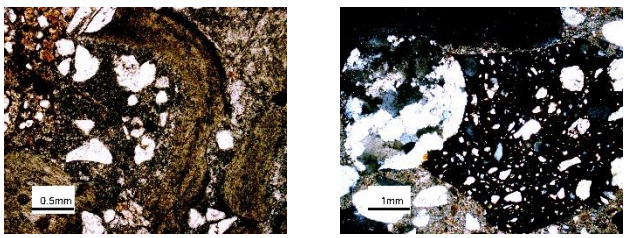

Fig. 4. Representative petrographic microscope images of shells and ceramic material under NC (crossed nickels) and NP (parallel nickels)

Optical microscopy of thin sections confirmed the presence of siliceous aggregates in all samples, with quartz being the predominant mineral. Quartzite (ALC1B, ALC4I), quartz sandstone (ALC2E), and amphiboles (ALC2I, ALC3) were also identified. Quartz aggregates generally displayed sub-angular to rounded morphologies, suggesting a fluvial origin. Samples ALC6 and ALC7 showed the highest lithological diversity, including ceramic particles, argillite, marble, and granite. Rounded lime nodules were also detected in several samples (e.g., ALC1B, ALC2I, ALC5, ALC6I). Potassic feldspars, especially microcline, were identified in ALC5.

X-ray diffraction (XRD) analysis (tab.2) revealed that the predominant crystalline phases are quartz, calcite, and potassic feldspars (orthoclase, sanidine, microcline, anorthoclase). These were common to all samples. Plagioclase feldspars (albite, anorthite, labradorite) and micas (muscovite, biotite, phlogopite, chlorite) appeared in moderate to trace amounts. Secondary minerals such as illite, kaolinite, dolomite, gypsum, and sodium nitrate occurred sporadically.

	CRYSTALLINE PHASES IDENTIFIED BY XRD								
			FELDSPAR						
SAMPLE	Quartz	Calcite	Potassic	Plagioclase	Micas	Clays	Dolomite	Nitratine	Gypsum
ALC1A	++	V	++	+	V	-	-	-	-
ALC1B	++	V	++	+	V	-	-	-	-
ALC2E	++	+	++	V	-	-	-	-	-
ALC2I	+	+	+++	V	V	-	-	V	-
ALC3	++	+	+++	-	V	-	-	-	-
ALC4E	++	+	+++	-	-	-	-	-	-
ALC4I	+	V	+	++	+	-	-	-	-
ALC5	+	V	++	++	-	-	-	-	-
ALC6E	+	+	+	+	+	-	+	-	-
ALC6I	++	V	+	-	+++	-	-	-	-
ALC7E	++	++	++	-	+	-	V	-	-
ALC7I	+++	+	+	+	-	-	-	-	-
ALC8E	+	++	+	-	-	++	-	-	-
ALC9E	+	+	+	V	+	V	+	-	-
ALC9I	+	+	+	+	+	-	-	-	V
ALC10R	+	V	+++	V	V	-	-	-	-
ALC10T	+	+	+++	++	-	-	-	V	-
ALC11EE	+	++	+	-	V	V	+	++	-
ALC11EI	++	+	++	-	+	-	-	+	-
ALC11I	+	V	+	-	+	-	-	V	V

(intensity peaks: dominant +++, major ++, minor +, trace V, not detected -)

Tab. 2. Mineralogical characterization of the GF of the mortar samples under study

Samples from each zone showed similar mineralogical compositions, indicating the consistent use of aerial lime mortars across the site. For instance, ALC1A and ALC1B shared a mineralogical profile of quartz, calcite, K-feldspars (microcline, orthoclase), plagioclase (albite, anorthite), and muscovite. Gismondine and microperthite were identified in several samples, notably in Zones 2 and 5.

Thermogravimetric analysis (TGA) revealed significant mass losses between 600–900°C across most samples, confirming the dominance of calcitic aerial lime as binder. The decomposition of calcium carbonate, correlating with

CO_2 release, was used to quantify $CaCO_3$ content. For example, samples such as ALC3, ALC4E, and ALC9E showed high carbonate content (20–51%), while ALC4I, ALC6I, and ALC7E revealed lower values (<9%). Samples ALC1A, ALC1B, and ALC2I, which included biogenic material (e.g., shell fragments), exhibited mass losses associated with these constituents, potentially skewing binder-to-aggregate ratio calculations (Tab.3).

SAMPLE	MASS LOSS/% 600-900°C	CALCIUM CARBONATE CONTENT/%
ALC1A	6.66	15.3
ALC7E	5.89	1.3
AL9E	21.65	49.6

Tab. 3. TG/DTG temperature ranges (°C) and mass losses (%) of some individual samples.

Additional thermal reactions were observed. Gypsum-related mass losses occurred near 150°C in ALC9I (Fig.5) and ALC11I, aligned with XRD detections. DTG curves showed dolomite decomposition peaks around 650°C in several samples (e.g., ALC7EXT, ALC8EXT, ALC10T), consistent with mineralogical data.

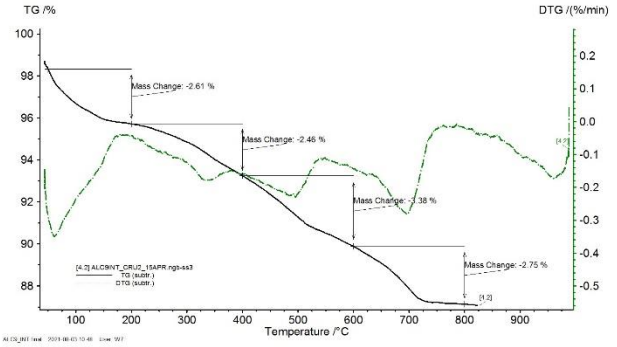

Fig. 5. TG/DTG temperature ranges (°C) and mass losses (%) of sample ALC9I.

Scanning Electron Microscopy with Energy Dispersive Spectroscopy (SEM-EDS) analysis from three distinct zones, revealed unique microstructural and compositional characteristics. Mortars from Zones 2 and 3 showed a predominantly calcitic binding phase, with aggregates of quartz and potassium feldspar that were sub-angular to sub-rounded in shape (Fig.6). In contrast, the Zone 1 mortar (sample ALC1A) exhibited significant heterogeneity. Its upper part contained quartz and feldspar aggregates, while the lower section's binding phase also included clay minerals associated with fragments of calcitic lime (Fig.7). Furthermore, the ALC6E sample from Zone 3 was notable for its greater heterogranularity and the presence of small, calcitic aggregates.

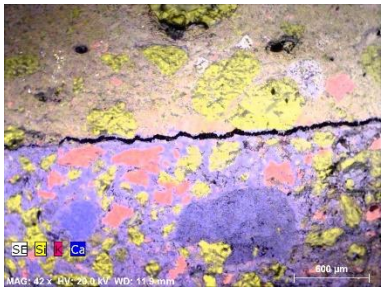

Fig. 6. Sample ALC-2E: EDS elemental distribution for the elements Si, K, and Ca. Ceramic fragment (top) contacting mortar and lime nodule.

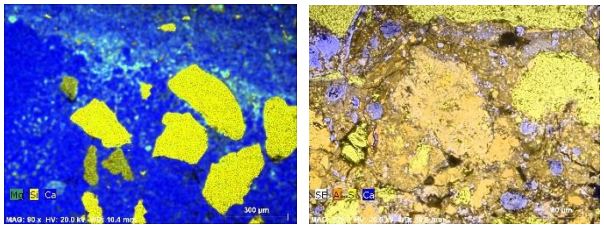

Fig. 7. Shows ALC1A (upper/outer) EDS elemental distribution for elements Si, Ca and Mg. Evidencing the calcitic binding phase. Shows ALC1A (bottom/inner part) EDS elemental distribution for Si, Ca, and Al elements.

The simplified composition of the mortars can be estimated on the basis of the method developed by Hanna Jedrzejewska for ancient lime mortars]. The components of mortars are considering in this method: aggregates (percentage of insoluble residue in acid attack (IR)), carbonates (percentage of carbonates estimated by TGA) and acid "soluble fraction" (percentage of soluble compounds in acid, without carbon dioxide generation) The soluble fraction content (SF) will be expressed as a percentage and calculated using equation (2).

$$SF(\%) = 100 - (IR\,(\%) + Carbonates(\%))$$

The results showed that most samples (72.2-84%) (Fig.8) had a high percentage of insoluble residue, with a soluble-to-insoluble ratio ranging from 1:3 to 1:5. Some samples from Zones 3, 4, and 5, associated with recent interventions, showed higher soluble fraction values, suggesting the presence of neoformation or hydraulic compounds.

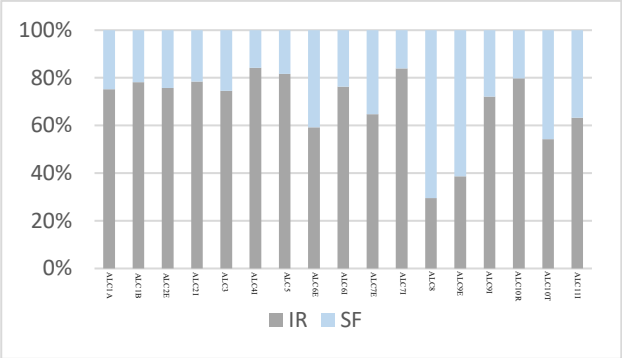

Fig. 8. The mass percentages of insoluble residue and soluble fraction of the studied mortars samples, obtained by acid attack.

Following the acid attack, granulometric analysis of the isolated aggregates showed a dominant fraction with a particle size between 250µm and 500µm. Microscopic observation confirmed a predominance of **quartz** and **feldspar** grains, which were sub-rounded to sub-angular in shape.

IV. DISCUSSION

Based on the results obtained through optical microscopy (OM), X-ray diffraction (XRD), thermogravimetric analysis (TGA), and scanning electron microscopy with energy-dispersive spectroscopy (SEM-EDS), the rendering mortars sampled from the defensive walls of Alcácer do Sal are characterized by a calcitic lime binder. The consistent identification of calcite by XRD, along with TGA data showing significant mass losses in the 600–900°C range, and the detection of calcium in elemental EDS maps, supports the interpretation of an aerial lime binder of calcitic nature.

Furthermore, acid attack with hydrochloric acid (HCl 1:3) revealed a soluble carbonate fraction, which may overestimate the actual amount of lime due to the presence of biogenic materials such as shell fragments and carbonate-rich aggregates. This potential overvaluation highlights the need to use complementary methodologies such as Petrographic point-count analysis of thin sections. Regarding the aggregates used in the mortars, siliceous sand is predominant, with occasional occurrences of potassium feldspars and micas. In some samples, particularly from zone 1, ceramic and shell fragments were identified, while in zones 2 and 3, lithic fragments such as quartzite, sandstone, marble, and mudstone were present. The diversity of inclusions indicates variability in raw material selection or availability at different construction phases or sectors of the wall.

The simplified binder-to-aggregate ratios estimated from the samples vary widely. Islamic mortars show consistent ratios of 1:6 to 1:8, which may reflect standardized production practices. However, the broader set of samples reveals ratios ranging from 1:3 to 1:8, with extreme cases as low as 1:1 and as high as 1:19. This high variability may result from the incorporation of carbonate-rich aggregates and shell fragments—leading to overestimated binder proportions—or from post-depositional leaching of carbonates, which can cause underestimations. It is also important to consider that some deviations may stem from sample representativeness limitations, especially given the fragmentary nature of the collected specimens.

In terms of raw material provenance, the sands used in the Islamic-period mortars are likely to originate from alluvial deposits in the region, as suggested in earlier geological surveys [Antunes, 1983]. Specifically, fine to medium sands from the Alcácer Formation are mentioned as being exploited during that period. The recurrent presence of shell fragments supports a marine Miocene influence in the sand sources. As for the lime binder, given the scarcity of stone in the region, Jurassic limestones or breccia from the Arrábida region are considered the most probable raw materials for the production of the aerial lime found in the older mortars, which show no evidence of dolomitic material.

The analytical methods employed in this study did not confirm the presence of materials reported in prior DGEMN documentation, as outlined in section 3.4.1. Nonetheless, the current data provides a consistent view of the technological practices, raw materials, and variability in mortar composition in the defensive structures of Alcácer do Sal, reflecting both standardized techniques and local adaptations.

V. STRATEGY DEFINITION

Situated within a transitional landscape between the Serra da Arrábida, the Tróia Peninsula, and the Sado estuary, the city of Alcácer do Sal currently extends along the river, with the hilltop occupied by the former fortress, a few scattered dwellings, agricultural plots, and ongoing archaeological excavations.

This study aims to enhance the architectural heritage of the city walls by proposing conservation strategies that combine preservation with public accessibility. A key outcome is the design of an interpretative path that connects the remaining wall segments with the surrounding landscape, offering historical insight into the site.

The deterioration observed is primarily due to a lack of maintenance and prolonged exposure to environmental conditions, especially rainwater and wind. Proposed corrective measures include removal of degraded render and its replacement with lime mortar (1:# ratio) using compatible, washed aggregates; partial reconstruction of masonry and missing copings; vegetation removal using appropriate herbicides; and drainage improvements along

adjacent terrain. In Zone 5, drainage is proposed through 10 cm diameter pipes spaced every 1.5 m, placed 20 cm from the wall base, filled with rolled aggregates wrapped in geotextile.

The proposed 1 km route includes pathways, stairs, and observation points that guide visitors through the site and highlight the relationship between the built structure and the landscape. Materials such as metal and wood were selected for their visual integration and reversibility. Metal elements in contact with lime mortars are protected with neoprene sheets to prevent corrosion.

VI. CONCLUSION

The study focused on the current condition and past interventions of Alcácer do Sal's defensive walls, aiming to inform future conservation strategies. While some southern and western segments near the Pousada show evidence of maintenance—likely from the 1995 intervention—other areas, particularly to the north and east, exhibit advanced degradation. These zones, built in military rammed earth, deteriorated more rapidly due to exposure to rain and lack of protective elements like copings and renders.

Moisture infiltration was identified as a major cause of decay, particularly in thick stone masonry walls without proper drainage. This leads to salt migration, surface efflorescence, and detachment of renders. Vegetation growth further contributes to structural damage.

Material analysis confirmed the use of air lime mortars with quartz and feldspar aggregates, with some regional variations. The presence of lime grains in rammed earth supports its classification as military taipa. The wall's construction reflects a strategic use of materials adapted to different defensive needs, particularly in the more exposed southern front.

To preserve and activate this heritage, the study proposes a cohesive intervention strategy that links and protects remaining wall segments, ensuring their accessibility and historical continuity.

REFERENCES

[1] P. Adriano, A. Santos Silva, R. Veiga, J. Mirão, & A. E. Candeias, "Microscopic characterisation of old mortars from the Santa Maria Church in Évora", *Materials Characterization*, 2008.

[2] J. Appleton, "Tecnologias de reabilitação em edifícios antigos, dos conventos às pousadas", *Jornal dos Arquitectos*, n.º 147, Lisboa, 1997.

[3] H. Baranha, "Património Cultural: conceitos e critérios fundamentais", IST Press e ICOMOS-Portugal, 2016.

[4] A. Bakolas, A. Biscontin, A.E. Zendri, "Characterization of structural byzantine mortars by thermogravimetric analysis", *Thermochimica Acta*, 321, 1998.

[5] P. Bruno, P. Faria, A. Candeias, J. Mirão, "Earth mortars from on pre-historic habitat setlements in south Portugal. Case studies", *J. Iberian Archaeology*, 13, 2010.

[6] C. Cabral, "Património Cultural Imaterial: Convenção da Unesco e seus Contextos", Edições 70, 2011.

[7] J.V. Caldas, M. Alçada, M.I.T. Grilo, "Caminhos do Património 1929-1999", DGEMN, Lisboa, 1999.

[8] J. Chagas, "O Castelo de Alcácer do Sal e a utilização da taipa militar durante o domínio almóada [Dissertação de Mestrado]", Universidade de Évora, 1995.

[9] F. Choay, "As questões do Património. Antologia para um combate", Edições 70, 2011.

[10] V. Correia, "Escavações realizadas na Necrópole Pré-Romana de Alcácer do Sal em 1926 e 1927", *Obras. Volume IV, Estudos Arqueológicos*, Universidade de Coimbra, Coimbra, p. 169-179, 1972.

[11] M. Földvári, "Handbook of the Thermogravimetric System of Minerals and Its Use in Geological Practice", Vol. 213, *Central European Geology*, Butapest: GFeological Institute of Hungary, 2011.

[12] H. Guillaud & H. Houben, "Traité de Construction en Terre", Editions Parenthéses, Marseille, 1989.

[13] J. Lanas, J. L. Pérez Bernal, M. A. Bello, e J. I. Alvarez Galindo, "Mechanical properties of natural hydraulic lime-based mortars", *Cement and Concrete Research*, 34(12), pp. 2191-2201, 2004.

[14] C. Mileto & F. Vegas, "La restauración de la tapia en la Península Ibérica – critérios, técnicas, resultados y perspectivas", *Argumentum*, 2014.

[15] D. R. Moorehead, "Cementation by the carbonation of hydrated lime", *Cement Concrete Research*, 16, pp. 700-708, 1986.

[16] M. Pereira, "Do Castelo à Ribeira: a urbanização de Alcácer (de finais do século XIII ao início de Quinhentos)", in L. Oliveira (Ed.), *Comendas Urbanas das Ordens Militares*, Edições Colibri, pp. 121-192, 2016.

[17] M. P. Riccardi, P. Duminuco, C. Tomasi, P. Ferloni, "Thermal (1998) Microscopy and X-Ray, Studies on Some Ancient Mortars", *Thermochimica Acta*, vol 321, 1998.

[18] B. H. Stuart, "Analytical Techniques in Materials Conservation", John Wiley & Sons, England, 2007.

[19] M. Veiga, A. Fragata, A. Velosa, A. Magalhães, G. Margalha, "Lime-based mortars: viability for use as substitution renders in historical buildings", *International Journal of Architectural Heritage*, 4, 2010.

[20] P. Vitrúvio, "Tratado de Arquitectura", tradução do latim por M. Justino Maciel, I.S.T., Lisboa, 2006